



Synthesis of isoquinolinone-based tetracycles as poly (ADP-ribose) polymerase-1 (PARP-1) inhibitors

Hee-Kyung Rhee^a, So Yun Lim^b, Mi-Ja Jung^b, Youngjoo Kwon^b, Myung-Hwa Kim^c, Hea-Young Park Choo^{b,*}

^a Department of Biological Science, Sookmyung Women's University, Seoul 140-742, Republic of Korea

^b College of Pharmacy and Division of Life and Pharmaceutical Sciences, Ewha Womans University, Seoul 120-750, Republic of Korea

^c R&D Center, Jeil Pharmaceutical Co. Ltd, Kyunggi-do 449-861, Republic of Korea

ARTICLE INFO

Article history:

Received 8 July 2009

Revised 7 September 2009

Accepted 10 September 2009

Available online 15 September 2009

Keywords:

PARP-1

Isoquinolinone

Cytotoxic potentiation

ABSTRACT

The isoquinolinone-based tetracyclic compounds were designed and synthesized and their PARP-1 inhibitory activity was evaluated. Most of synthesized compounds showed fairly good activity. Also the most active compound 6 showed its activity on potentiation of anticancer agents, temozolamide and etoposide, by 1.7 times, respectively.

© 2009 Elsevier Ltd. All rights reserved.

1. Introduction

Poly (ADP-ribose) polymerase (PARP) is a nuclear enzyme in eukaryotic cells which is involved in the regulation of many cellular functions. It becomes activated in the response to DNA damage, and has been implicated in DNA repair.¹ The PARP family includes the proteins of PARP-1, PARP-2, PARP-3, Tankyrase-1, Tankyrase-2, TipARP and vPARP. Among the PARP family PARP-1 is one of the most abundant proteins and has been believed the main isoform.² PARP comprises a 42 kDa N-terminal DNA binding domain containing two zinc fingers (FI and FII), a 22 kDa automodification domain, and a 54 kDa C-terminal catalytic domain.^{3,4} Following binding of PARP to damaged site in DNA, this results in a highly negatively charged target, which in turn leads to the unwinding and repair of the damaged DNA through the base excision repair pathway. Initially, the enzyme brings about the transfer of the ADP-ribose fragment of NAD⁺ to target acceptor proteins including the automodification domain of PARP. Overactivation of PARP results in depletion of NAD⁺ and leads to cellular death by necrosis.⁵

PARP activity is increased in tumor cells, leading to prevent from apoptosis caused by DNA-damaging agent. PARP is essential for the excision repair pathways. The PARP inhibitor interacts with PARP catalytic fragment through two hydrogen bonds between its amide group and the peptide backbone of Gly863 and the oxygen atom of the side chain of Ser904 in the same way as the nicotinamide moiety of NAD⁺.³

It is clear that the majority of PARP inhibitors are based on the benzamide as pharmacophore, which mimics the nicotinamide moiety of NAD⁺.³ Five PARP inhibitors are currently under the clinical oncology trials (AG014699 by Pfizer;^{6,7} KU59436 by AstraZeneca/KUDOS; BSI-201 by Bipar, INO-1001 by Inotek/Genentech; GPI 21016 by MGI pharma). ABT-888 in Abbott laboratories^{8,9} is expected to enter clinical trials. INO-1001 is currently in phase 2 trial for cardiovascular indication. It is also being studied in combination therapy in metastatic melanoma and glioma with temozolamide in phase 1 trial and as a single agent in cancer for breast cancer type 1 and 2 susceptibility protein (BRCA1 and BRCA2) deficient tumors.¹

In this research, the isoquinolinone-based tetracyclic analogs with modification of Inotek's compound **3** (Fig. 1)¹⁰ were designed and synthesized to find out their activity on potentiation of anticancer agents temozolamide and etoposide.

2. Results and discussion

2.1. Chemistry

In this work, the synthetic route reported by John Huffman in 1985 was adopted (Scheme 1).¹¹ The different amine components possessing various heterocycles such as substituted pyridine, pyrimidine, and pyrazine were employed. The reaction of methyl or halogen substituted 2-aminopyridine, *o*-phthaldehydic acid and cyanide ion gave substituted-pyrido[2',1':2,3]imidazo[4,5-*c*]isoquinolin-5-(6*H*)-one as reported. When amino-pyrimidine,

* Corresponding author. Fax: +82 2 3277 2821.

E-mail address: hypark@ewha.ac.kr (Hea-Young Park Choo).

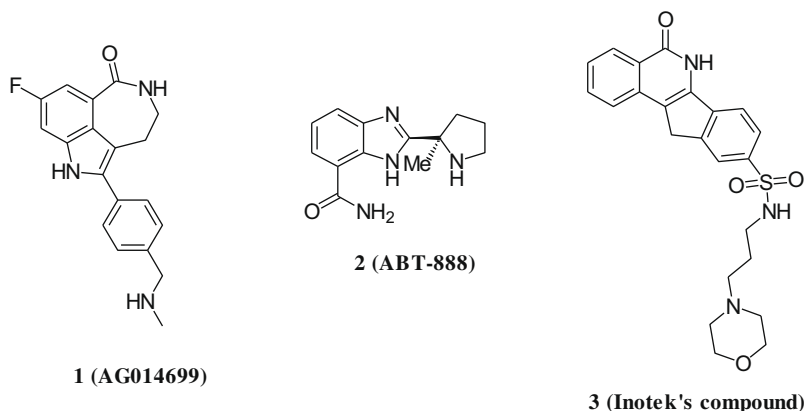
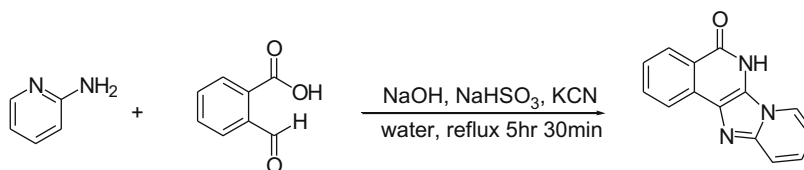


Figure 1. PARP-1 inhibitors.



Scheme 1. Synthesis of isoquinolinone-based tetracycles.

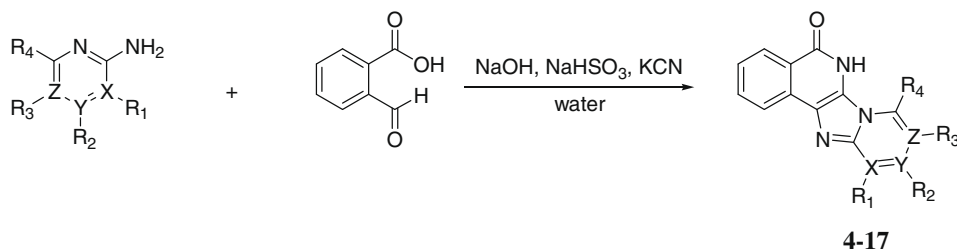
isoquinoline, or pyrazine instead of 2-aminopyridine were employed the yield were decreased to 15–30%.

The one-pot synthesis of similar compounds were also reported by a tandem three component reaction of heteroaromatic amines, methyl 2-formylbenzoate and *t*-butyl isonitrile, followed by TFA-mediated lactamization via intramolecular aminolysis of an adjacent esters.¹²

2.2. PARP-1 inhibitory activity

Among the 14 compounds prepared, most of compounds showed PARP inhibitory activity (Table 1). The compounds with methyl group at R₂ (**6** and **16**) showed very good activity. The introduction of halogen at R₂ or R₃ showed good activity but the effect was less than that of methyl group. The compounds substi-

Table 1
PARP-1 inhibitory activities of isoquinolinone-based tetracyclic analogs



Compound	R ₁	R ₂	R ₃	R ₄	X	Y	Z	IC ₅₀ (μM)
DPO								10.82 ± 0.28
3								0.036 ± 0.002
4	H	H	H	H	C	C	C	0.85 ± 0.40
5	CH ₃	H	H	H	C	C	C	3.31 ± 0.51
6	H	CH ₃	H	H	C	C	C	0.47 ± 0.32
7	H	H	CH ₃	H	C	C	C	4.27 ± 0.86
8	H	H	H	CH ₃	C	C	C	>100
9	H	H	Cl	H	C	C	C	14.85 ± 8.73
10	H	H	Br	H	C	C	C	12.09 ± 5.07
11	H	Cl	H	H	C	C	C	5.87 ± 0.07
12	H	CH ₃	H	CH ₃	C	C	C	>100
13	H	—	H	H	C	N	C	3.23 ± 2.07
14	—	H	H	H	N	C	C	5.78 ± 0.11
15			H	H	C	C	C	4.11 ± 0.96
16	—	CH ₃	H	H	N	C	C	0.56 ± 0.11
17	H	OCH ₃	H	H	C	C	N	>100

Table 2

DU145 Cell inhibitory activities of isoquinoline-based tetracyclic analogues at 10 μ M in MTT assay

Compound	% Inhibition
Adriamycin	70.3 \pm 3.7
Etoposide	72.1 \pm 3.6
Camptothecin	69.4 \pm 4.0
4	7.9 \pm 4.0
5	9.1 \pm 3.0
6	0 \pm 0.0
7	19.2 \pm 2.7
8	25.6 \pm 5.2
9	0.2 \pm 2.2
10	6.8 \pm 1.8
11	11.4 \pm 4.3
12	38.5 \pm 7.5
13	18.7 \pm 3.6
14	14.2 \pm 3.2
15	25.5 \pm 4.6
16	27.7 \pm 4.0
17	0 \pm 0.0

tuted with methyl group at R₄ position (**8** and **12**) showed no activity.

The introduction of more nitrogen on ring showed different activity depends on the position of nitrogen: nitrogen at X or Y (**13**, **14**, and **16**) was good for activity, but at Z (**17**) resulted in the loss of activity.

All the synthesized compounds had low cytotoxicity on human prostate tumor cell line (DU145) measured by MTT assay at 10 μ M as shown in Table 2. Therefore these compounds can be used as potentiating agents for chemotherapeutic drugs.

2.3. Effect of PARP-1 inhibitor on potentiating cytotoxicity of DNA-damaging antitumor agent

PARP inhibitors sensitize tumor cell to cytotoxic therapy. PARP inhibitor therapy may increase more effective in patients who have tumor with specific DNA repair defects or who take therapeutics which inhibit other DNA repair pathway.¹

Compounds **6** and **16** were selected to test whether they can potentiate cytotoxicity of DNA-damaging antitumor agent. Compound **8** was used as a negative control because it showed no PARP-1 inhibitory activity (Table 1). The activity of selected PARP-1 inhibitors as potentiators of cytotoxicity of antitumor agent was evaluated in vitro by treating HCT116 (human colon tumor cell line) with increasing concentration of two antitumor agents, the DNA methylating agent, temozolomide and the topoisomerase II inhibitor, etoposide, in the presence of a PARP-1 inhibitor at fixed concentration. Compound **6** enhanced the cytotoxicity induced by temozolomide as well as that caused by etoposide (Table 3).

Compound **16** had similar PARP-1 inhibitory activity to compound **6** (Table 1) but did not show the potentiation effect on DNA-damaging antitumor agents as much as compound **6** (Table 3). Compound **8** showed no activity on PARP-1 inhibition and further reduced the activity of temozolomide and etoposide. Even though compound **6** did not show great PARP-1 inhibitory activity, it was noticeable that **6** demonstrated the possibility to enhance cytotoxicity of DNA-damaging antitumor agent by co-treatment.

Recently, it has been reported that PARP-1 inhibitor, ADZ2281 decreased tumor size without toxicity in BRCA1 deficient breast cancer model mouse.¹² BRCA1 dysfunction is related to cause the triple-negative breast cancer (ERBB2-negative and hormone receptor-negative breast cancer). Target-specific drugs aiming for ERBB2-overexpressing and hormone receptor-positive breast cancer have been developed and used while no drugs targeting for triple-negative breast cancer are available. The triple-negative breast

Table 3

The potentiation effect on temozolomide and etoposide activity by selected PARP-1 inhibitors in HCT116 human tumor cell line

Compound	IC ₅₀ ^a (μ M)	PF ₅₀ ^b
Temozolomide	4.34 \pm 0.44	
Temozolomide + 8	14.01 \pm 3.26	
Temozolomide + 6	2.59 \pm 0.22	1.7
Temozolomide + 16	4.04 \pm 0.20	1.1
Etoposide	14.39 \pm 1.86	
Etoposide + 8	> 50	
Etoposide + 6	8.53 \pm 1.00	1.7
Etoposide + 16	12.14 \pm 0.60	1.2

^a Each data point represents mean \pm S.D. from at least three independent experiments.

^b The cytotoxic potentiation factor (PF₅₀) of PARP-1 inhibitor was expressed as the ratio of the IC₅₀ for cells treated with the cytotoxic agent alone, to the IC₅₀ of cells exposed to cytotoxic agent in the presence of PARP-1 inhibitor. Thus a PF₅₀ value of 1.0 indicates no effect and bigger PF₅₀ value is better potentiators of DNA-damaging antitumor agent cytotoxicity.¹⁴

cancer patients account for 15% of all breast cancer patients and respond to anticancer drug with worse survival rate than other types of breast cancer.¹³ Therefore it is important to develop therapeutic molecules against the triple-negative breast cancer. The result obtained from the present study may pave the way to design and develop effective PARP-1 inhibitor as a therapeutic molecule for triple-negative breast cancer.

3. Conclusion

The 14 isoquinolinone-based tetracyclic compounds were designed and synthesized as PARP-1 inhibitor. Most of synthesized compounds showed good PARP-1 inhibitory activity with IC₅₀ values of 0.4–6 μ M. When the cytotoxicity of most active compound **6** was assayed with anticancer agent temozolomide or etoposide, it showed the potentiation of cytotoxicity of anticancer agents by 1.7 times.

4. Experimental

4.1. Materials and methods

Melting points were measured on an electrothermal disital melting point (Büchi, Germany) without calibration. ¹H NMR spectra (DMSO-*d*₆) were recorded on Varian NMR AS and Varian Unity Inova 400 MHz NMR spectrometers. Chemical shifts were reported in parts per million (δ) units relative to the solvent peak. The ¹H NMR data were reported as peak multiplicities: s for singlet; d for doublet; t for triplet; and m for multiplet. Coupling constants were recorded in hertz. MS spectra were measured using JMS-Hx 110/110A. Reactions were checked with TLC (Merck precoated 60F254 plates). Spots were detected by viewing under a UV light. Reagents were of commercial grade and were purchased from Sigma–Aldrich Co., Merck, Ducksan Pure chemical Co.

4.2. General procedure for preparation of isoquinolin-5-one derivatives

A total of 0.04 g (1 mmol) of sodium hydroxide in 2 mL of water was mixed with 0.15 g (1 mmol) of phthaldehydic acid and when the mixture became solution, 0.104 g (1 mmol) of sodium bisulfite was added. This mixture was heated on a steam bath for 30 minutes then 0.11 g (1 mmol) of substituted-pyridine, pyrazine or pyrimidine was added. The mixture was heated for 1 h and potassium cyanide 0.104 g (1.6 mmol) was added and the mixture was heated for an additional 4 h. The mixture was cooled then acidified with acetic acid (CAUTION: HCN). Ice was added during

acidification, to keep the mixture cool. The resulting solid was filtered off, washed with water and dried.

4.2.1. Pyrido[2',1':2,3]imidazo[4,5-c]isoquinolin-5-(6H)-one (4)¹²

Yellow solid (44%), mp >300 °C; ¹H NMR (DMSO-*d*₆) δ 12.58 (s, br, 1H), 8.66 (d, *J* = 6.0 Hz, 1H), 8.34 (d, *J* = 7.6 Hz, 1H), 8.29 (d, *J* = 8.0 Hz, 1H), 7.88 (t, *J* = 7.4 Hz, 1H), 7.67 (d, *J* = 9.6 Hz, 1H), 7.60 (t, *J* = 8.0 Hz, 1H), 7.30 (t, *J* = 8.8 Hz, 1H), 7.62 (t, *J* = 6.4 Hz, 1H). ¹³C NMR (DMSO) δ 160.91, 142.44, 133.51, 133.07, 128.85, 127.03, 125.39, 123.87, 122.17, 118.12, 112.65. HR-FABMS Calcd for C₁₄H₉N₃O (M+H)⁺: 236.0824. Found: 236.0821.

4.2.2. 11-Methyl-6H-pyrido[2',1':1,2]imidazo[5,4-c]isoquinolin-5-one (5)¹²

Yellow solid (52%), mp >300 °C; ¹H NMR (DMSO-*d*₆) δ 12.82 (s, br, 1H), 8.52 (d, *J* = 6.8 Hz, 1H), 8.34 (d, *J* = 8.0 Hz, 2H), 7.86 (t, *J* = 7.4 Hz, 1H), 7.58 (t, *J* = 9.4 Hz, 1H), 7.11 (d, *J* = 6.8 Hz, 1H), 6.93 (t, *J* = 6.8 Hz, 1H), 2.71 (s, 3H). ¹³C NMR (DMSO) δ 160.93, 142.94, 133.45, 133.17, 128.80, 127.53, 126.88, 123.86, 122.21, 121.59, 112.65, 17.38. HR-FABMS Calcd for C₁₅H₁₁N₃O (M+H)⁺: 250.0980. Found: 250.0977.

4.2.3. 10-Methyl-6H-pyrido[2',1':1,2]imidazo[5,4-c]isoquinolin-5-one (6)

Yellow solid (82%), mp >300 °C; ¹H NMR (DMSO-*d*₆) δ 12.23 (s, br, 1H), 8.55 (d, *J* = 7.2 Hz, 1H), 8.33 (d, *J* = 8.4 Hz, 1H), 8.26 (d, *J* = 8.0 Hz, 1H), 7.86 (t, *J* = 8.0 Hz, 1H), 7.57 (t, *J* = 8.0 Hz, 1H), 7.43 (s, 1H), 6.88 (d, *J* = 7.2 Hz, 1H), 2.45 (s, 3H). ¹³C NMR (DMSO) δ 160.00, 142.29, 135.36, 132.71, 132.49, 128.10, 126.05, 124.95, 123.53, 122.87, 122.37, 121.44, 115.42, 114.55, 21.07. HR-FABMS Calcd for C₁₅H₁₁N₃O (M+H)⁺: 250.0980. Found: 250.0981.

4.2.4. 9-Methyl-6H-pyrido[2',1':1,2]imidazo[5,4-c]isoquinolin-5-one (7)

Yellow solid (70%), mp >300 °C; ¹H NMR (DMSO-*d*₆) δ 12.15 (s, br, 1H), 8.40 (s, 1H), 8.30 (d, *J* = 7.6 Hz, 1H), 8.24 (d, *J* = 7.6 Hz, 1H), 7.84 (t, *J* = 7.6 Hz, 1H), 7.56 (t, *J* = 7.6 Hz, 1H), 7.51 (d, *J* = 10.6 Hz, 1H), 7.16 (d, *J* = 10.6 Hz, 1H), 2.33 (s, 3H). ¹³C NMR (DMSO) δ 161.49, 141.53, 133.17, 128.87, 128.25, 126.58, 124.67, 123.62, 121.97, 121.51, 121.07, 117.49, 18.60. HR-FABMS Calcd for C₁₅H₁₁N₃O (M+H)⁺: 250.0980. Found: 250.0979.

4.2.5. 8-Methyl-6H-pyrido[2',1':1,2]imidazo[5,4-c]isoquinolin-5-one (8)

Yellow solid (40%), mp >300 °C; ¹H NMR (DMSO-*d*₆) δ 11.72 (s, br, 1H), 8.51 (d, *J* = 7.6 Hz, 1H), 8.35 (d, *J* = 8.0 Hz, 1H), 7.92 (t, *J* = 7.4 Hz, 1H), 7.68 (t, *J* = 7.8 Hz, 1H), 7.58 (d, *J* = 9.6 Hz, 1H), 7.34 (t, *J* = 7.2 Hz, 1H), 6.77 (d, *J* = 6.4 Hz, 1H), 3.20 (s, 3H). ¹³C NMR (DMSO) δ 167.98, 144.99, 134.74, 131.26, 131.08, 130.52, 126.89, 126.20, 125.92, 125.08, 122.82, 121.63, 114.92, 111.50, 19.87. HR-FABMS Calcd for C₁₅H₁₁N₃O (M+H)⁺: 250.0980. Found: 250.0979.

4.2.6. 9-Chloro-6H-pyrido[2',1':1,2]imidazo[5,4-c]isoquinolin-5-one (9)

Yellow solid (51%), mp >300 °C; ¹H NMR (DMSO-*d*₆) δ 12.80 (s, br, 1H), 8.86 (s, 1H), 8.34 (d, *J* = 7.2 Hz, 1H), 8.26 (d, *J* = 7.6 Hz, 1H), 7.89 (t, *J* = 7.2 Hz, 1H), 7.72 (d, *J* = 9.6 Hz, 1H), 7.61 (t, *J* = 7.6 Hz, 1H), 7.32 (d, *J* = 9.6 Hz, 1H). HR-FABMS Calcd for C₁₄H₈N₃OCl (M+H)⁺: 270.0434. Found: 270.0432.

4.2.7. 9-Bromo-6H-pyrido[2',1':1,2]imidazo[5,4-c]isoquinolin-5-one (10)

Yellow solid (33%), mp >300 °C; ¹H NMR (DMSO-*d*₆) δ 12.69 (s, br, 1H), 8.84 (s, 1H), 8.33 (d, *J* = 7.6 Hz, 1H), 8.23 (d, *J* = 7.6 Hz, 1H),

7.82 (t, *J* = 6.8 Hz, 1H), 7.61 (d, *J* = 8.8 Hz, 1H), 7.55 (t, *J* = 7.2 Hz, 1H), 7.32 (d, *J* = 10.0 Hz, 1H). ¹³C NMR (DMSO) δ 168.51, 167.33, 150.97, 141.27, 141.11, 138.42, 133.47, 131.17, 129.19, 123.75, 123.21, 122.75, 112.06. HR-FABMS Calcd for C₁₄H₈N₃OBr (M+H)⁺: 315.9910. Found: 315.9895.

4.2.8. 10-Chloro-6H-pyrido[2',1':1,2]imidazo[5,4-c]isoquinolin-5-one (11)

Yellow solid (60%), mp >300 °C; ¹H NMR (DMSO-*d*₆) δ 12.93 (s, br, 1H), 8.66 (d, *J* = 7.2 Hz, 1H), 8.34 (d, *J* = 7.6 Hz, 1H), 8.26 (s, 1H), 7.91–7.86 (m, 2H), 7.61 (t, *J* = 8.0 Hz, 1H), 7.13 (d, *J* = 7.2 Hz, 1H). ¹³C NMR (DMSO) δ 160.87, 142.05, 133.58, 132.83, 130.30, 128.83, 127.26, 124.80, 124.52, 122.23, 116.73, 113.85, 112.52. HR-FABMS Calcd for C₁₄H₈N₃OCl (M+H)⁺: 270.0434. Found: 270.0437.

4.2.9. 8,10-Dimethyl-6H-pyrido[2',1':1,2]imidazo[5,4-c]isoquinolin-5-one (12)

Yellow solid (53%), mp >300 °C; ¹H NMR (DMSO-*d*₆) δ 11.66 (s, br, 1H), 8.47 (d, *J* = 8.4 Hz, 1H), 8.33 (d, *J* = 8.8 Hz, 1H), 7.89 (t, *J* = 6.8 Hz, 1H), 7.65 (t, *J* = 7.2 Hz, 1H), 7.35 (s, 1H), 6.64 (s, 1H), 3.15 (s, 3H), 2.39 (s, 3H). ¹³C NMR (DMSO-*d*₆) δ 156.51, 146.03, 138.17, 137.38, 131.69, 131.60, 126.47, 122.20, 114.81, 114.74, 113.64, 113.58, 20.02. HR-FABMS Calcd for C₁₆H₁₃N₃O (M+H)⁺: 264.1137. Found: 264.1138.

4.2.10. 6H-Pyrimido[4',3':1,2]imidazo[5,4-c]isoquinolin-5-one (13)¹²

Yellow solid (8%), mp >300 °C; ¹H NMR (DMSO-*d*₆) δ 13.01 (s, br, 1H), 9.15 (s, 1H), 8.61 (d, *J* = 3.2 Hz, 1H), 8.37 (d, *J* = 7.2 Hz, 1H), 8.34 (d, *J* = 10.0 Hz, 1H), 7.96 (d, *J* = 4.8 Hz, 1H), 7.93 (t, *J* = 6.8 Hz, 1H), 7.67 (t, *J* = 7.2 Hz, 1H). ¹³C NMR (DMSO) δ 160.62, 143.74, 136.49, 133.30, 131.91, 128.47, 128.27, 127.54, 124.66, 121.82, 116.09. HR-FABMS Calcd for C₁₃H₈N₄O (M+H)⁺: 237.0776. Found: 237.0775.

4.2.11. 6H-Pyrimido[1',2':1,2]imidazo[5,4-c]isoquinolin-5-one (14)¹²

Yellow solid (9%), mp >300 °C; ¹H NMR (DMSO-*d*₆) δ 12.86 (s, br, 1H), 9.01 (d, *J* = 6.8 Hz, 1H), 8.58 (s, 1H), 8.36 (d, *J* = 8.0 Hz, 1H), 8.32 (d, *J* = 7.2 Hz, 1H), 7.91 (t, *J* = 7.2 Hz, 1H), 7.64 (t, *J* = 7.6 Hz, 1H), 7.18–7.16 (m, 1H). ¹³C NMR (DMSO-*d*₆) δ 160.91, 150.73, 144.87, 133.66, 132.82, 132.08, 132.04, 128.87, 127.57, 127.54, 122.53, 109.02, 108.99. HR-FABMS Calcd for C₁₃H₈N₄O (M+H)⁺: 237.0776. Found: 237.0774.

4.2.12. 6H-Naphto[2',1':1,2]imidazo[5,4-c]isoquinolin-5-one (15)

Yellow solid (8%), mp >300 °C; ¹H NMR (DMSO-*d*₆) δ 12.90 (s, br, 1H), 8.59 (d, *J* = 7.6 Hz, 1H), 8.51 (d, *J* = 7.2 Hz, 1H), 8.34 (d, *J* = 10.0 Hz, 2H), 7.89 (t, *J* = 8.0 Hz, 2H), 7.70 (m, 2H), 7.58 (t, *J* = 7.6 Hz, 1H), 7.36 (d, *J* = 7.6 Hz, 1H). ¹³C NMR (DMSO) δ 161.18, 156.65, 140.06, 137.58, 136.76, 133.56, 133.16, 132.43, 129.72, 128.81, 127.51, 125.19, 123.80, 123.36, 121.88, 121.30, 118.05, 111.01. HR-FABMS Calcd for C₁₃H₁₁N₃O (M+H)⁺: 286.0980. Found: 286.0983.

4.2.13. 10-Methyl-pyrimido[1',2':1,2]imidazo[5,4-c]isoquinolin-5-one (16)

Yellow solid (20%), mp >300 °C; ¹H NMR (DMSO-*d*₆) δ 12.63 (s, br, 1H), 8.90 (d, *J* = 6.8 Hz, 1H), 8.34 (d, *J* = 7.6 Hz, 1H), 8.28 (d, *J* = 7.6 Hz, 1H), 7.89 (t, *J* = 6.8 Hz, 1H), 7.60 (t, *J* = 6.8 Hz, 1H), 7.06 (d, *J* = 6.8 Hz, 1H), 2.58 (s, 3H). HR-FABMS Calcd for C₁₄H₁₀N₄O (M+H)⁺: 251.0933. Found: 251.0930.

4.2.14. 10-Methoxy-6H-pyrimido[3',4':1,2]imidazo[5,4-c]isoquinolin-5-one (17)

Yellow solid (15%), mp >300 °C; ^1H NMR (DMSO- d_6) δ 12.74 (s, br, 1H), 9.31 (s, 1H), 8.34 (d, J = 8.0 Hz, 1H), 8.25 (d, J = 7.6 Hz, 1H), 7.89 (t, J = 7.2 Hz, 1H), 7.61 (t, J = 7.6 Hz, 1H), 6.90 (s, 1H), 3.93 (s, 3H). ^{13}C NMR (DMSO) δ 162.54, 160.91, 160.26, 149.60, 146.43, 138.02, 133.32, 132.44, 129.64, 128.65, 128.50, 122.87, 122.34, 55.80. HR-FABMS Calcd for $\text{C}_{14}\text{H}_{10}\text{N}_4\text{O}_2$ ($\text{M}+\text{H}$) $^+$: 267.0882. Found: 267.0884.

4.3. PARP-1 enzyme assay

The IC_{50} of PARP inhibitor compounds was determined by using Trevigen PARP inhibition kit (Gaithersburg, USA). The assay was performed in 384-well small volume microplates (Greiner Bio-one, Frickenhausen, Germany) according to modified methods as follows.¹⁵

The PARP-1 enzyme assay is set up in a volume of 12 microliters. Wells were coated with diluted histones (12 μL /well, 1:10 dilution), followed by the incubation at 25 °C for 2 h. After washing the plates four times with PBS, all the liquid was removed following each wash by tapping plate onto paper towels. To block the nonspecific signal, the wells were blocked by adding the Strep-diluent (Trevigen, 12 μL /well) and incubated at 25 °C for 1 h. The plates were washed four times with PBS, serial dilutions of compound was added (3 μL /well). Then, the diluted PARP-1 enzyme was added to each well (0.12 unit/well), except in wells for the negative control and combined with 6 μL per well of 2 \times PARP cocktail. The reaction was allowed to proceed for 30 min at 25 °C. After washing four times with PBS, add streptavidin-linked peroxidase (Strep-HRP, 1:1000 dilution) to detect the extent of ribosylation and incubated at 37 °C for 30 min. Then, the plates were washed four times with PBS, followed by addition of TACS-Sapphire substrate (12 μL /well) and allowed to develop the color for 10 min. Finally, the reaction was stopped by adding 0.2 N HCl (12 μL /well) and optical densities were read at 450 nm by Wallac EnVisionTM (Perkin-Elmer Oy, Turku, Finland). All the data points were determined in triplicate and the data were analyzed using the SigmaPlot 10 (Systat Software Inc., USA).

4.4. Cytotoxic potentiation assay

HCT116 (human colorectal carcinoma cell line) was cultured in the medium of RPMI 1640 (Hyclone, USA) supplied with 10% FBS (Hyclone, USA) and incubated in 5% CO_2 incubator at 37 °C. Cells were seeded in 96-well plates at a density of 3×10^4 cells per well

and incubated overnight in 0.1 mL of medium. On day 2, culture medium in each well was exchanged with 0.1 mL aliquots of medium containing graded concentrations of temozolomide (Sigma, USA) and etoposide (Sigma, USA), respectively, in the absence and presence of 0.5 μM concentration of PARP-1 inhibitors. On day 4, each well was added with 5 μL of the cell counting kit-8 solution (Dojindo, Japan) then incubated for additional 4 h under the same condition. The absorbance of each well was determined by an Automatic Elisa Reader System (Bio-Rad 3550) 450 nm wavelength. For determination of the IC_{50} values, the absorbance readings at 450 nm were fitted to the four-parameter logistic equation.

Acknowledgment

This investigation was supported by Jeil Pharmaceutical Co.

References and notes

- Ratnam, K.; Low, J. A. *Clin. Cancer Res.* **2007**, *13*, 1383.
- Ame, J.-C.; Spencehauer, C.; de Murcia, G. *BioEssays* **2004**, *26*, 1148.
- Jagtap, P.; Szabo, C. *Nat. Rev. Drug Disc.* **2005**, *4*, 421.
- Griffin, R. J.; Srinivasan, S.; Bowman, K.; Calvert, A. H.; Curtin, N. J.; Newell, D. R.; Pemberton, L. C.; Golding, B. T. *J. Med. Chem.* **1998**, *41*, 5247.
- Haince, J.-F.; Rouleau, M.; Hendzel, M. J.; Masson, J.-Y.; Poirier, G. G. *Trends Mol. Med.* **2005**, *11*, 456.
- Plummer, R.; Jones, C.; Middleton, M.; Wilson, R.; Evans, J.; Olsen, A.; Curtin, A.; Boddy, A.; McHugh, P.; Newell, D.; Harris, A.; Johnson, P.; Steinfeldt, H.; Dewji, R.; Wang, D.; Robson, L.; Calvert, H. *Clin. Cancer Res.* **2008**, *14*, 7917.
- Thomas, H. D.; Calabrese, C. R.; Batey, M. A.; Canan, S.; Hostomsky, Z.; Kyle, S.; Maegley, K. A.; Newell, D. R.; Skalitzy, D.; Wang, L.-Z.; Webber, S. E.; Curtin, N. J. *Mol. Cancer Ther.* **2007**, *6*, 945.
- Penning, T. D.; Zhu, G.-D.; Gandhi, V. B.; Gong, J.; Liu, X.; Shi, Y.; Klinghofer, V.; Johnson, E. F.; Donawho, C. K.; Frost, D. J.; Bontcheva-Diaz, V.; Bouska, J. J.; Osterling, D. J.; Olson, A. M.; Marsh, K. C.; Luo, Y.; Giranda, V. L. *J. Med. Chem.* **2009**, *52*, 514.
- Donawho, C. K.; Luo, Y.; Luo, Y.; Penning, T. D.; Bauch, J. L.; Bouska, J. J.; Bontcheva-Diaz, V. D.; Cox, B. F.; DeWeese, T. L.; Dillehay, L. E.; Ferguson, D. C.; Ghoreishi-Haack, N. S.; Grimm, D. R.; Guan, R.; Han, E. K.; Holley-Shanks, R. R.; Hristov, B.; Idler, K. B.; Jarvis, K.; Johnson, E. F.; Kleinberg, L. R.; Klinghofer, V.; Lasko, L. M.; Liu, X.; Marsh, K. C.; McGonigal, T. P.; Meulbroek, J. A.; Olson, A. M.; Palma, J. P.; Rodriguez, L. E.; Shi, Y.; Stavropoulos, J. A.; Tsurutani, A. C.; Zhu, G.-D.; Rosenberg, S. H.; Giranda, V. L.; Frost, D. J. *Clin. Cancer Res.* **2007**, *13*, 2728.
- Jagtap, P. G.; Baloglu, E.; Southan, G. J.; Mabley, J. G.; Li, H.; Zhou, J.; Van Duzer, J.; Salzman, A. L.; Szabo, C. *J. Med. Chem.* **2005**, *48*, 5100.
- Paolini, J. P.; Palopoli, F. P.; Lendvay, L. J.; Huffman, J. J. *Heterocycl. Chem.* **1987**, *24*, 549.
- Che, C.; Xiang, J.; Wang, G.-X.; Fathi, R.; Quan, J.-M.; Yang, Z. J. *Comb. Chem.* **2007**, *9*, 982.
- Onitilo, A. A.; Engel, J. M.; Greenlee, R. T.; Mukesh, B. N. *Clin. Med. Res.* **2009**, *1/2*, 4.
- Bowman, K. J.; White, A. W.; Golding, B. T.; Griffin, R. J.; Curtin, N. J. *Br. J. Cancer* **1998**, *78*, 1269.
- Lee, B. H. *Methods Find Exp. Clin. Pharmacol.* **2005**, *27*, 617.